AAPS PharmSciTech, Vol. 13, No. 4, December 2012 (© 2012)
DOI: 10.1208/s12249-012-9852-x

Research Article

A Feasibility Study on Pellet Coating Using a High-Speed Quasi-continuous Coater

Christine Cahyadi,[1] Jackson Jie Sheng Koh,[1] Zhi Hui Loh,[1] Lai Wah Chan,[1] and Paul Wan Sia Heng[1,2]

Received 3 May 2012; accepted 10 September 2012; published online 21 September 2012

Abstract. Pellet coating is traditionally carried out using the Wurster coater. This study investigated the feasibility of pellet coating in a newly developed coater built with a unique airflow system, the Supercell™ coater (GEA Pharma Systems, UK). A full factorial design study was carried out to evaluate the influences of the spray rate of the coating dispersion, batch size of the pellet load, pellet size fraction and plenum pressure of the fluidizing air on the color coating of pellets in the Supercell™ coater. Results showed that pellets could be successfully coated using the Supercell™ coater. Higher plenum pressures and lower spray rates were found to minimize pellet agglomeration during coating. Although coating efficiencies were comparable amongst the different pellet size fractions, larger batch sizes of pellets were coated with higher efficiencies. Process optimization was carried out for each pellet size fraction and a large batch size (120 g) in combination with a high plenum pressure (1,500 mm WC) were deemed optimal. Optimal spray rates differed according to pellet size fraction and a lower spray rate was required for smaller pellets. Pellet flow patterns observed during coating were dependent on the pressure drop across the fluidized load. A 'swirling' pellet flow pattern was generally observed at coating conditions which led to optimal outcomes.

KEY WORDS: fluid bed; fluidization; pellet coating; pellet flow patterns; pressure drop; process optimization; Supercell™ coater.

INTRODUCTION

In the pharmaceutical industry, multi-particulates such as pellets are typically coated for the purpose of producing controlled or sustained release dosage forms (1). Compared to tablets, coated pellets offer more predictable drug release patterns unaffected by the rates of gastric emptying. They also reduce the risk of dose-dumping should there be defects on the coats of some unit particulates (2).

Pellet coating is traditionally carried out using the Wurster coater, a bottom-spray fluid bed coater (1,3). However, the Wurster coater has been associated with problems of pellet agglomeration during the coating process. This was partly attributed to the dense flow of pellets within the central partition column, where the close proximity of pellets with respect to one another often results in extensive agglomeration (3,4). Unpredictable airflow patterns in the partition gap, defined as the gap between the base of the central partition column and the air distribution plate, further exacerbated the problem of agglomeration (5). Therefore, the height of the partition gap needs to be carefully selected in Wurster coating to ensure smooth pellet flow patterns (6) and appropriate pellet flow rates (7).

The Supercell™ coater (GEA Pharma Systems, UK) is a newly developed high-speed bottom-spray fluid bed coater designed for the coating of articles, in particular tablets. Tablets are continuously coated as multiple small batches in a quasi-continuous manner. The Supercell™ tablet coating process has been successfully optimized (8) and the Supercell™ coater was shown to be capable of coating tablets with a high degree of uniformity and accuracy (9,10). However, the Supercell™ coater has not been studied for the coating of multi-particulates such as pellets. In contrast to the Wurster coater, the airflow within the Supercell™ coater is engineered with a unique airflow system which swirls the particles at high velocity through the coating zone, thereby omitting the need of a central partition column (5). The movement of particles in the coating zone of the Supercell™ coater during a tablet coating process is illustrated in Fig. 1. The ducts that encircle the spray nozzle modify the atomizing air in a way that a low-pressure upward swirling airflow pattern is created during coating.

In a previous study (4), the use of a swirling airflow in a bottom-spray fluid bed coater was shown to be able to impart sufficient shear forces to the pellet load to break any transiently formed liquid bridges which precedes agglomeration. It was thus hypothesized that the Supercell™ coater, in view of its unique swirling airflow pattern, may be able to reduce the problem of pellet agglomeration *via* a similar mechanism. This study was conducted to investigate the feasibility of pellet coating using the Supercell™ coater. The major factors

[1] GEA-NUS Pharmaceutical Processing Research Laboratory, Department of Pharmacy, Faculty of Science, National University of Singapore, 18 Science Drive 4, Singapore, 117543, Singapore.
[2] To whom correspondence should be addressed. (e-mail: phapaulh@nus.edu.sg)

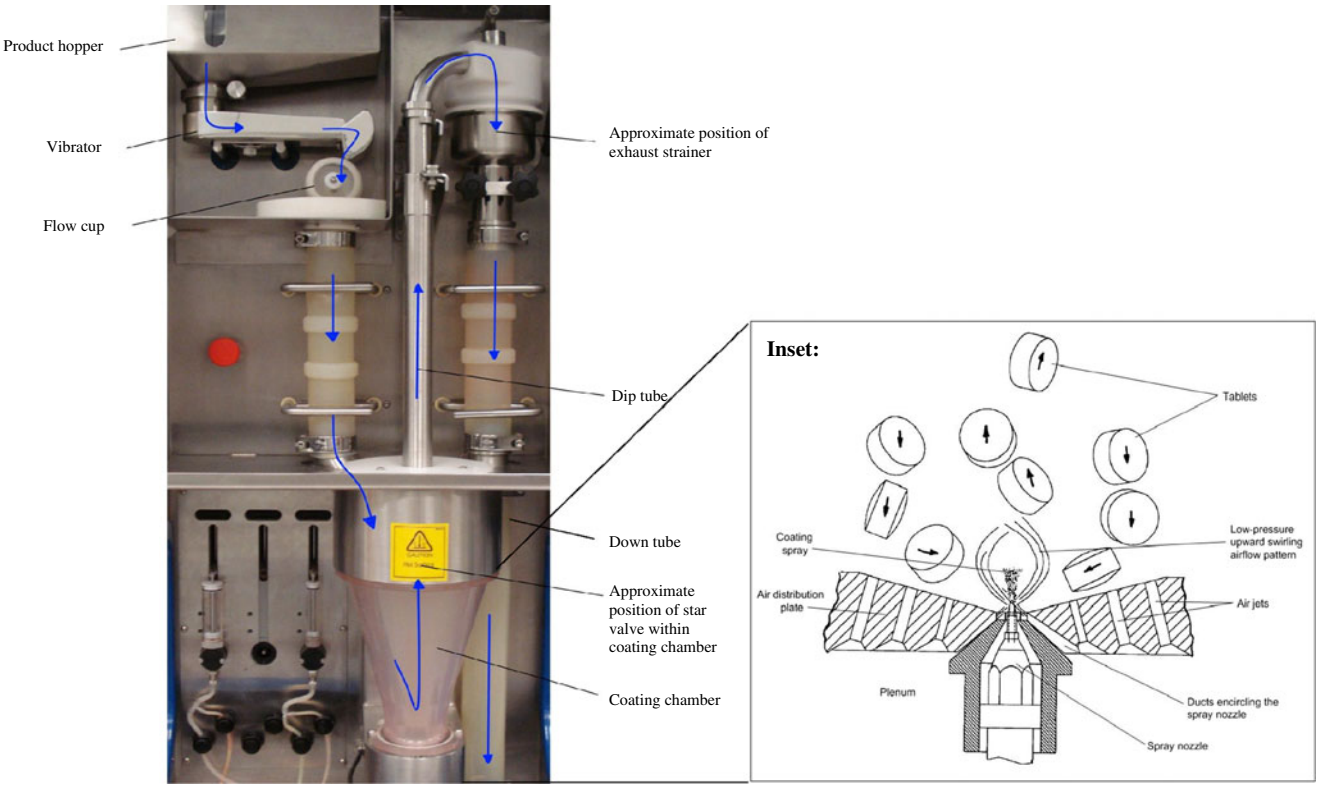

Fig. 1. Photo showing the equipment controls of the Supercell™ coater. *Arrows* indicate the direction from pellet loading to pellet collection. *Inset* (reproduced from reference (5)): schematic diagram of the tablet coating process. *Arrows* indicate the direction of tablet movement

influencing the pellet coating process were evaluated and process conditions were optimized for the production of quality pellet coats with low degree of agglomeration and high coating efficiency.

MATERIALS AND METHODS

Study Design

The thermodynamic aspects of tablet coating were considered in the study design. The Supercell™ coater leverages on airflow patterns and process parameters to ensure appropriate balance of the system's thermodynamics. A 3^4 full factorial design was carried out to study the effects of four factors on the pellet coating process. Specifically, these factors included the spray rate of the coating dispersion, batch size of the pellet load, plenum pressure contributed by the fluidizing air and size fraction of pellets. Each factor was varied at three levels (Table I). Any thermodynamic imbalance would result in differences in yield, coating efficiency and degree of agglomeration. The atomizing air pressure and inlet air temperature during the coating process were kept constant at two bars and 80°C, respectively. Centre samples were included for estimation of the experimental error, and were triplicated for each pellet size fraction. A total of 90 coating runs were carried out.

Preparation of Pellet Cores

Pellet cores were prepared *via* extrusion–spheronization and comprised 65%, *w*/*w* lactose (Pharmatose 450M, DMV International, Netherlands), 25%, *w*/*w* microcrystalline cellulose (Avicel PH101, FMC BioPolymer, Ireland) and 10%, *w*/*w* paracetamol (Wenzhou Pharm Factory, China). Three processing conditions were employed for extrusion–spheronization to obtain pellets of different size fractions. The three process conditions employed are summarized in Table II. Accurately weighed quantities of the individual materials amounting to a total of 1 kg of powder mixture were first mixed. Wet massing was then carried out (KM250, Kenwood Electronics, UK) for 6 min by the addition of an appropriate amount of water to the powder mixture. The wet mass was then fed into the extruder (E140, Aeromatic Fielder, UK) fitted with an extruder screen of the appropriate aperture size. The extrudates formed were subsequently loaded into the spheronizer (S320, Aeromatic Fielder, UK) and spheronized for 7 min at a suitable tip speed. The pellets produced were oven-dried overnight at 60°C and equilibrated at 25°C/50% RH in a temperature- and humidity-controlled room before coating.

Table I. Factors Varied and the Quantitative Values of the Levels at Which They Are Varied

Factors	Low level	Intermediate level	High level
Pellet size fraction (mm)	1.00–1.40	1.40–2.00	2.00–2.80
Spray rate (mL/min)	4	6	8
Batch size (g)	40	80	120
Plenum pressure (mm WC[a])	500	1,000	1,500
Approximate airflow rate (m^3/h)	16.5	24.0	28.5

[a] Millimeters water column

Table II. Conditions Employed for Extrusion–Spheronization

Extrusion–spheronization	Process conditions		
	1	2	3
Water content of wet mass (%, *w*/*w*)	41.0	42.5	45.0
Extruder screen aperture size (mm)	1.5	3.0	3.6
Spheronizer tip speed (m/min)	469.12	423.90	334.41

The dried pellets were subsequently passed through a nest of sieves with aperture sizes ranging from 1.00 to 2.80 mm with the aid of an automated sieve shaker operating at an amplitude of 1.0 for 5 min (VS1000, Retsch, Germany). The three different size fractions of pellets employed for subsequent coating were 1.00–1.40 mm, 1.40–2.00 mm and 2.00–2.80 mm.

Characterization of Pellet Cores

The size and shape of the pellet cores were evaluated by image analysis. Images of the uncoated pellets were captured using a stereomicroscope (Olympus SZ61, Olympus Corp., Japan) under 0.67× objective. The images were processed using an image analysis software (Image-Pro Plus, MediaCybernetics, USA) to determine the aspect ratio, minimum diameter, maximum diameter, and mean diameter of the pellets. Approximately 500 pellets were analyzed for each pellet size fraction.

Table III shows the measured characteristics of the uncoated pellet cores. The pellets produced were spherical with aspect ratios ranging from 1.09 to 1.12. The 1.40–2.00 mm pellet size fraction had the widest size distribution as evidenced by a large relative standard deviation of the mean pellet diameter.

Coating of Pellets

Color coating of the pellets was carried out using the Supercell™ coater in accordance with the study design. The coating dispersion comprised 9%, *w*/*w* Opadry Red (03B15211, Colorcon Inc, China), a hypromellose-based formulation, prepared in deionized water. Chlorpheniramine maleate (Merck, Singapore) was also dissolved in the coating dispersion to attain a concentration of 1%, *w*/*w*. After completing the addition of all ingredients, the coating dispersion was stirred (SS10, Stuart Scientific, UK) for 30 min prior to coating and agitation was maintained throughout the coating process. Pellets were coated to achieve a theoretical weight gain of 3%, *w*/*w*.

Observation of Pellet Flow Patterns

The flow patterns of pellets during the coating process were captured using a video recorder (GZ-MG335, JVC Limited, Japan).

Determination of Yield

At the end of the coating process, the pellets were equilibrated at 25°C/50% RH in a temperature- and humidity-controlled room for at least 24 h before measurements were made. The yield (Yd) for each coating run was subsequently calculated using the following equation:

$$Yd(\%) = \frac{Total\ weight\ of\ pellets\ collected\ after\ coating}{Batch\ size\ of\ load + Weight\ gain\ from\ coating} \times 100 \quad (1)$$

Determination of Degree of Agglomeration

After coating, pellets from the 1.00–1.40 mm, 1.40–2.00 mm and 2.00–2.80 mm size fractions were passed through sieves of aperture sizes 1.70 mm, 2.80 mm and 3.35 mm, respectively. The oversized fractions of coated pellets were classified as agglomerates and weighed to calculate the degree of agglomeration (Agg) according to the following equation:

$$Agg(\%) = \frac{Weight\ of\ pellets\ retained\ on\ the\ sieve}{Total\ weight\ of\ pellets\ collected\ after\ coating} \times 100 \quad (2)$$

Determination of Pellet Loss

An overview of the equipment controls in Supercell™ coating is shown in Fig. 1. The star valve found at the top of the coating chamber had a perforated wall and an opening with flexible flaps. At the end of each coating run, the dip tube

Table III. Size and Shape Characteristics of Uncoated Pellet Cores

Pellet characteristics	Pellet size fraction (mm)		
	1.00–1.40	1.40–2.00	2.00–2.80
Aspect ratio	1.09 (±0.07)	1.10 (±0.09)	1.12 (±0.10)
Min. diameter (mm)	1.050 (±0.110)	1.363 (±0.227)	1.985 (±0.194)
Max. diameter (mm)	1.191 (±0.149)	1.567 (±0.304)	2.329 (±0.275)
Mean diameter (mm)	1.118 (±0.124)	1.460 (±0.257)	2.146 (±0.214)
RSD of mean diameter (%)	11.09	17.60	9.97
Total surface area in 200 mg sample (mm^2)	–	Smaller pellets, 606.14 (±0.29) Larger pellets, 338.20 (±0.17)	–

In parenthesis, ± standard deviation
RSD relative standard deviation

was lowered through the star valve to extract the coated pellets. The pellets would then pass through an exhaust strainer to filter the fines into the exhaust, before exiting *via* the down tube.

As the Supercell™ coater was originally developed for the coating of larger articles such as tablets; modifications were required to prevent the escape of pellets *via* the exhaust by fitting a woven mesh with aperture size smaller than 1.00 mm over the wall of the star valve and the exhaust strainer. During coating, a small proportion of pellets would escape to the exhaust *via* the gaps between the flexible flaps of the star valve opening. The latter could not be covered as this would obstruct the collection of the coated pellets *via* the dip tube. Small amounts of pellets were also observed to bypass the exhaust strainer and were lost to the exhaust.

All pellets collected after coating were examined visually. Uncoated or partially coated pellets were distinguishable from those well coated. Since the former was undesirable, it was considered as pellet loss. The proportion of pellet loss (PL) was calculated as follows:

$$PL(\%) = \frac{Weight\ of\ uncoated/partially\ coated\ pellets}{Total\ weight\ of\ pellets\ collected\ after\ coating} \times 100 \quad (3)$$

Determination of Coating Efficiency

The amount of chlorpheniramine maleate (CM) present in the pellet coats provided an indication of the amount of coating material deposited on the pellets. CM deposited was quantified using high-performance liquid chromatography (LC-2010C, Shimadzu, Japan).

Accurately weighed 200 mg of pellets collected after coating were immersed in 10 mL of ultrapure water (Direct-Q 3, Millipore Corp, USA) and sonicated (LC60H, Fisher Scientific, Singapore) for 1 min to dissolve and extract the drug. The resulting suspension was centrifuged (2–5, Sartorius, Germany) for 5 min at 4,000 rpm, and the supernatant was filtered through a 0.45 μm membrane filter (RC, Sartorius, Germany). For chromatographic analysis, a 100×4.6 mm reversed-phase C-18 column (BDS Hypersil, ThermoScientific, USA) was employed. The mobile phase, which consisted of methanol 10%, *v/v* in water, was maintained at a flow rate of 0.4 mL/min. The column oven was maintained at 40°C throughout the analysis and CM was detected at 264 nm. The retention time of CM was found to be approximately 2.01 min. Measurements were triplicated for each pellet batch. The coating efficiency (E_c) was estimated according to the following equation:

$$E_c(\%) = \frac{Amount\ of\ CM\ present\ in\ 200\ mg\ sample}{Theoretical\ amount\ of\ CM\ in\ the\ 200\ mg\ sample} \times 100 \quad (4)$$

For further analysis, the 1.40–2.00 mm pellet size fraction was separated into two sub-fractions consisting of smaller (1.40–1.70 mm) and larger (1.70–2.00 mm) pellets respectively to analyze the variation in drug deposition in a pellet size fraction of relatively wide size distribution. Table III shows the mean total surface area of the smaller and larger pellets in a 200 mg sample of pellets. Coating efficiency was expressed by the amount of CM deposited per unit surface area of pellet (DSA) for both the smaller pellets (DSA_{small}) and the larger pellets (DSA_{large}).

Statistical Analysis

A univariate general linear model (SPSS 16.0, IBM Corp, USA) was used to analyze the full factorial design at a 5% level of significance. Plots of the main effects were used to describe the change in response brought about by a change in the level of a factor. Independent-sample *t* test was used when two means were compared and one-way analysis of variance with Tukey's *post hoc* test was used when more than two means were compared.

RESULTS AND DISCUSSION

Factors Influencing Yield

Yd provides an indication of the amount of coating material deposited onto the pellets. Pellet size was found to exert the greatest influence on Yd, where an increase in pellet size led to an increase in Yd (Fig. 2). This suggested that the coater was more suitable for coating larger pellets or articles. However, coating efficiencies as determined by drug content deposited revealed a different trend (Section "Factors Influencing Coating Efficiency"). Small amounts of pellets were observed to bypass the star valve and the exhaust strainer. The lower Yd value for smaller pellets was attributed to the greater loss of smaller pellets to the exhaust. The larger pellets were less likely to bypass the exhaust strainer, leading to fewer pellet losses and higher Yd after coating.

Factors Influencing Degree of Agglomeration

Pellet agglomeration is brought about by the formation of stable bonds between discrete pellets. Shortly after their transit through the spray zone, the pellets may collide with one another, leading to the formation of transient liquid bridges at their points of contact. If the liquid bridges are strong enough

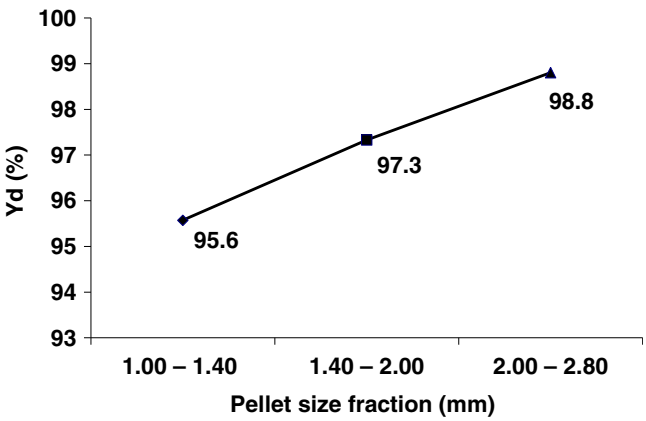

Fig. 2. Main effects plot of pellet size fraction on Yd. Pellet size fractions: (*black diamond*) 1.00–1.40 mm (*black square*) 1.40–2.00 mm (*black triangle*) 2.00–2.80 mm

to resist the shearing forces of the fluidizing air, subsequent drying may cause the formation of solid bridges between pellets resulting in the formation of agglomerates (6).

Analysis of the factorial design showed that plenum pressure exerted the greatest influence on Agg. For all three pellet size fractions, an increase in plenum pressure from 500 to 1,500 mm WC significantly ($p<0.05$) reduced Agg (Fig. 3a). At a plenum pressure less than 1,000 mm WC, the fluidizing air was unable to impart sufficient shear forces to break the liquid bridges formed between pellets. Furthermore, the drying capability of the air was diminished at lower pressure, with reduced airflow and reduced rate of evaporation. The thermodynamic imbalance led to prolonged sticky phase with more gradual drying of the coating material newly deposited on the pellet surfaces and brought about greater extents of agglomeration. When plenum pressure was increased beyond 1,000 mm WC, Agg decreased to negligible levels for all pellet size fractions. Spray rate was also found to significantly influence Agg ($p<0.05$) for all three pellet size fractions. As expected, Agg was higher with an increase in spray rate (Fig. 3b). However, batch size was found not to significantly influence Agg ($p=0.12$).

In addition to process parameters, the pellet size fraction used for coating also exerted a significant effect on Agg ($p<0.05$). The highest Agg was observed in the smallest size fraction of pellets (1.00–1.40 mm) (Fig. 3c). This was probably attributed to their larger specific surface area which increased the likelihood of pellet–pellet collisions (11). The Agg values of the 1.40–2.00 mm and 2.00–2.80 mm pellet size fractions were however comparable.

Factors Influencing the Proportion of Pellet Loss

The PL value ranged from 0 to 12.35% for all the coating runs (data not shown). Analysis of the factorial design showed that both batch size and plenum pressure significantly influenced PL ($p<0.05$). For all pellet size fractions, an increase in batch size and decrease in plenum pressure led to a decrease in PL (Fig. 4a and b). The loss of pellets through the star valve situated at the top of the coating chamber was affected not only by the physical size of the pellets but also the extent to which the pellets were fluidized. When the batch size was increased or the plenum pressure was decreased, the specific pellet fluidization energy decreased. Under these circumstances, the upper height of pellets being fluidized was reduced, thus less could escape through the star valve. As shown in Fig. 4c, PL increased significantly ($p<0.05$) when smaller pellets were used as they were more liable to slip through the gaps between the flexible flaps of the star valve opening. Spray rate did not have a significant effect on PL ($p=0.30$). This was probably due to its minimal influence on the extent of pellet fluidization.

Factors Influencing Coating Efficiency

Coating efficiency had been inferred from drug content as it reflected the amount of coating material deposited (12). From the factorial design analysis, batch size was found to exert the greatest influence on the coating efficiencies of all pellet size fractions ($p<0.05$). E_c was found to increase with increasing batch size (Fig. 5a). The increase in batch size led to a higher pellet concentration within the spray zone at any one

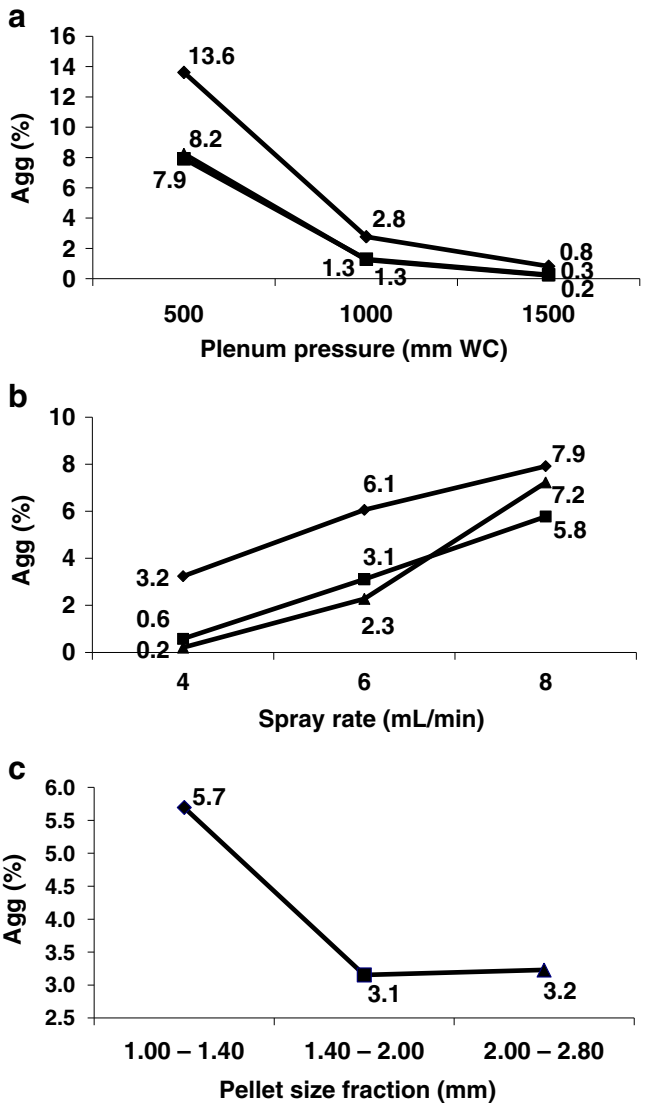

Fig. 3. Main effects plots of **a** plenum pressure, **b** spray rate and **c** pellet size fraction, on Agg. Pellet size fractions: (*black diamond*) 1.00–1.40 mm (*black square*) 1.40–2.00 mm (*black triangle*) 2.00–2.80 mm

time during coating. This increased the surface area available for coating material deposition and more importantly, enhanced the likelihood of contact between the atomized spray droplets and the pellets. Based on visual observations during the coating, the loss of coating material to the wall of the coating chamber was indeed more apparent when a small batch size (40 g) of pellets was coated. In addition, material loss arising from the spray-drying effect was likely to be higher when a smaller batch was coated.

Spray rate significantly affected the coating efficiency of the smallest size fraction (1.00–1.40 mm) of pellets ($p<0.05$), but exerted minimal influence on the coating efficiencies of the larger 1.40–2.00 mm ($p=0.50$) and 2.00–2.80 mm ($p=0.59$) pellet size fractions. For the 1.00–1.40 mm pellet size fraction, E_c decreased with an increase in spray rate (Fig. 5b). The increased spray rate led to over-wetting of the pellet surfaces, and this brought about coating material loss to the wall of the coating chamber when pellet–wall collisions occurred. The smallest pellet size fraction was most affected in view of their low pellet weight, which enabled higher fluidization and the

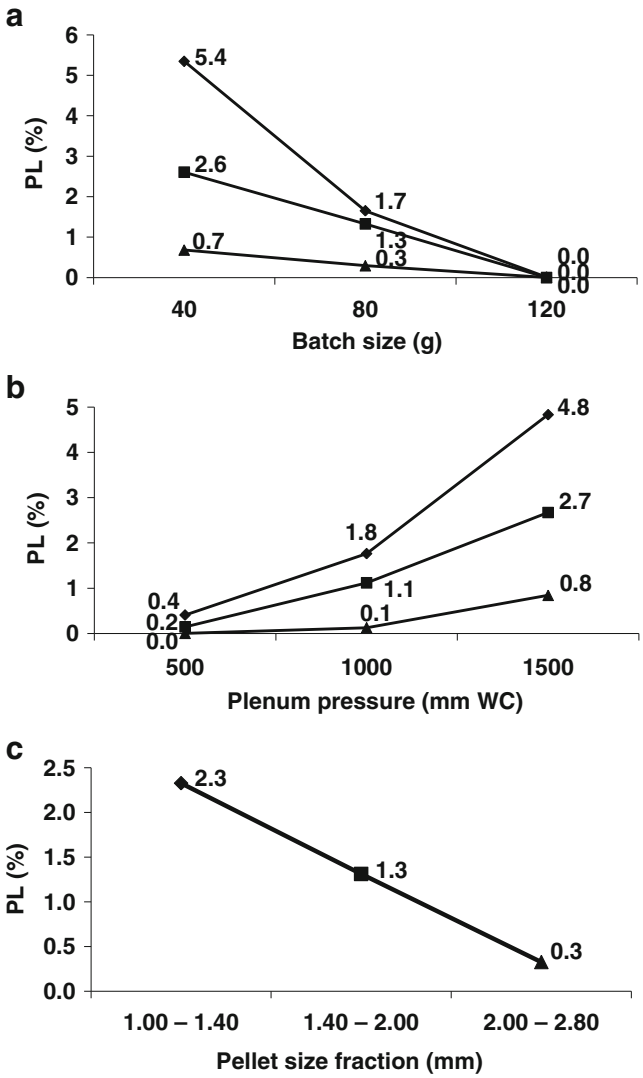

Fig. 4. Main effects plots of **a** batch size **b** plenum pressure **c** pellet size fraction on PL. Pellet size fractions: (*black diamond*) 1.00–1.40 mm (*black square*) 1.40–2.00 mm (*black triangle*) 2.00–2.80 mm

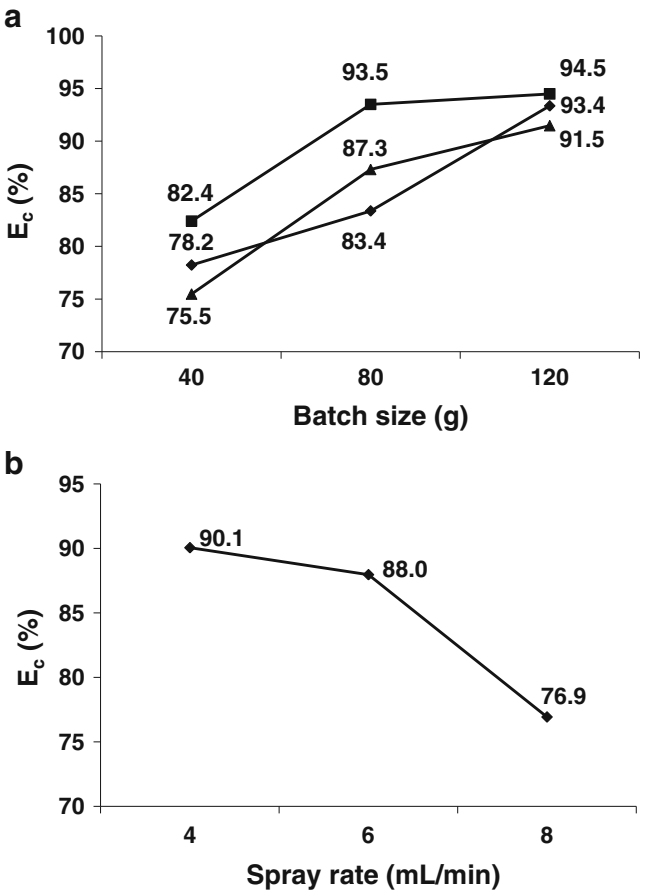

Fig. 5. Main effects plots of **a** batch size and **b** spray rate on E_c. Pellet size fractions: (*black diamond*) 1.00–1.40 mm, (*black square*) 1.40–2.00 mm and (*black triangle*) 2.00–2.80 mm

increased frequency of pellet–wall collisions. Plenum pressure did not exert a significant influence on the coating efficiencies ($p>0.05$) of all pellet size fractions.

An independent-samples *t* test was performed to investigate the effect of pellet size on coating efficiency by comparing the E_c between the 1.00–1.40 mm and 2.00–2.80 mm pellet size fractions. The 1.00–1.40 mm pellet size fraction had a mean E_c of 84.9±2.0% whereas the 2.00–2.80 mm pellet size fraction had a mean E_c of 85.1±1.6%. There was no significant difference between the E_c of the two pellet size fractions ($p=0.92$). This indicates that the drug content and hence, the amount of the coating material deposited was not markedly affected by the pellet size used in the Supercell™ coater. This was in contrast to the trend in coating efficiency based on Yd, where the larger pellets were shown to result in higher coating efficiency based on the approximation of coating weight gain (Fig. 2). The evaluation of drug content is a more accurate method of determining the coating efficiency of the coating process. The use of weight measurements is typically adequate for the estimation of coating efficiency. However, any loss of materials during the process will result in the underestimation of the coating efficiency. It should be noted that it is possible for the apparent E_c to increase when there is less pellet mass due to pellet loss during coating. However, there may also be increased losses due to spray-drying effects. The amount of material deposited on the pellets will eventually be dependent on the process conditions employed during coating

Further study was carried out to investigate the influence of pellet size on coating efficiency within the same batch of pellets. The coated 1.40–2.00 mm size fraction of pellets was divided into two fractions, comprising smaller and larger pellets respectively. This was carried out to investigate the impact of wide size distribution on drug deposition. Within the same size fraction, the mean DSA for the larger (DSA_{large}) and smaller (DSA_{small}) pellets were 0.98±0.02 μg/mm^2 and 1.41±0.03 μg/mm^2, respectively. Independent-samples *t* test showed that DSA_{small} was significantly lower than DSA_{large} ($p<0.05$), indicating that the smaller pellets received relatively less coating material deposition per unit surface area compared to their larger counterparts. This phenomenon has been reported in previous studies involving the Wurster coating of pellets with a wide size distribution (13,14). It was believed that the large disparities in pellet sizes led to varying degree of fluidization heights achieved during coating and also corresponded to variations in pellet coating cycle times. In addition, pellets of different sizes exhibit dissimilar velocities in their passage through the coating zone. This could also have resulted in the smaller pellets receiving less coating material

Table IV. R^2 Values of the Quadratic Models Fitted for Each Response

Pellet size fraction (mm)	Response	R^2 value of quadratic model (%)
1.00–1.40	SQRT Agg	84
	E_c	62
1.40–2.00	SQRT Agg	87
	DSA_{small}	62
	DSA_{large}	57
2.00–2.80	SQRT Agg	67
	E_c	76

(13). These explanations accounted for much of the differences in DSA of the different sized pellets coated in the Supercell™ coater. However, it should be noted that since the smaller pellets have a larger overall surface area for the same pellet weight, the total amount of drug deposited (595.6±67.4 μg) was found to be significantly higher than that of larger pellets (478.5±49.7 μg). A uniform pellet size distribution is important to ensure uniform drug deposition in Supercell™ coating. This issue is common in all types of fluidized bed processes.

Optimization of Pellet Coating

The pellet coating process was optimized (Minitab 15.1.1.0, Minitab Inc., USA) for two of the responses, Agg and coating efficiency. These two responses were selected as they were direct measures of product quality and process efficiency. Optimization was carried out separately for each pellet size fraction, resulting in three sets of optimized conditions.

The coating efficiencies of the pellets were expressed in terms of E_c for the 1.00–1.40 mm and 2.00–2.80 mm pellet size fractions and DSA for the 1.40–2.00 mm pellet size fraction. Prior to analysis, the Agg data obtained from all pellet size fractions were subjected to square-root transformation to obtain SQRT Agg. Response surface methodology was used to fit a quadratic model for each response which included all linear, squared and two-way interaction terms. It was important to recognize that the effect of changing a certain process parameter was always dependent on the relative levels of other parameters. Hence, responses were not easily predicted. Therefore, response surface methodology is an important tool to ensure that all variables were taken into consideration when considering the ideal settings for production. Table IV shows the R^2 values of the quadratic models fitted for each response. The models were checked for significance ($p<0.05$) and a non-significant lack-of-fit ($p>0.05$). Response optimizer settings were applied to minimize SQRT Agg and to maximize E_c or DSA. All responses were assigned the same weight and importance.

Predicted values were generated for each response according to the fitted models. Individual desirability (d) values were computed based on how close the predicted values approached the maximally desired response values. A composite desirability (D) value was calculated from all the d values according to their assigned weights and importance. The optimized condition would have the highest D value. The optimization plots generated for the different pellet size fractions and their respective D values are shown in Fig. 6. The optimized conditions are given in brackets.

For all the three pellet size fractions, a large batch size of about 120 g and a high plenum pressure of about 1,500 mm WC were deemed optimal for pellet coating. Based on the results discussed earlier, a large batch size was required to maximize the drug content whereas a high plenum pressure was needed to minimize agglomeration. On the other hand, the optimal spray rate predicted for the 1.00–1.40 mm pellet size fraction was different from the other two pellet size fractions. The smaller pellets exhibited a greater tendency to agglomerate and were therefore less able to withstand high spray rates. Furthermore, as previously discussed, drug content was significantly decreased by an increase in spray rate only within the 1.00–1.40 mm pellet size fraction.

Validation of Optimized Conditions

All three optimized conditions were identical or similar to the conditions already conducted within the factorial design. Therefore, separate validation runs were not carried out. Instead, the predicted responses of the optimized conditions

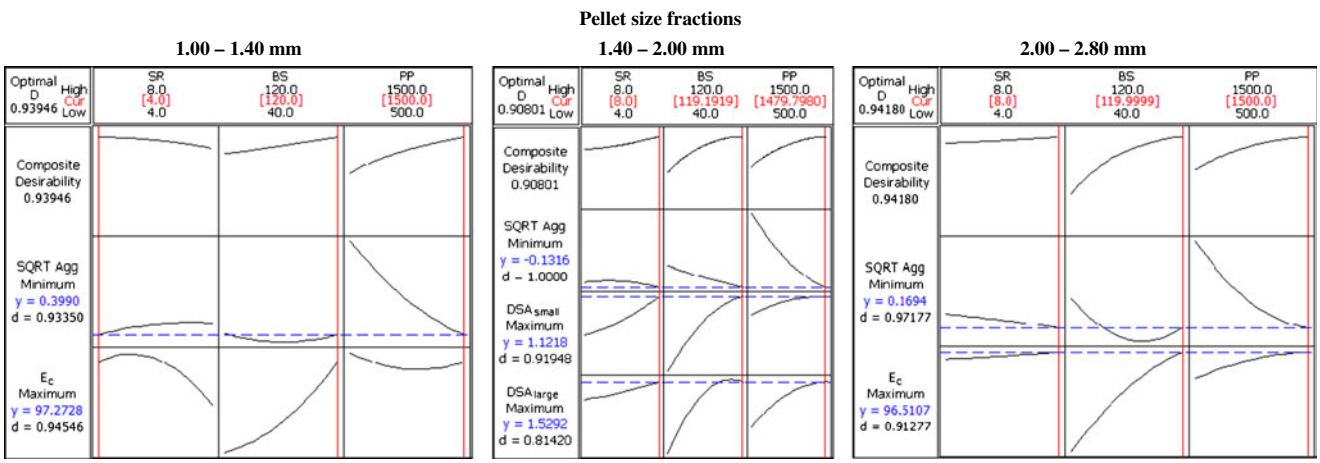

Fig. 6. Optimization plots for the respective pellet size fractions. Optimized conditions are shown in *brackets* while the predicted values of each response at the optimized condition are indicated by the *y*-values. (*D* composite desirability, *d* individual desirability, *SR* spray rate, *BS* batch size, *PP* plenum pressure, *SQRT Agg* square-root of the degree of agglomeration, E_c coating efficiency, *DSA* drug content per unit surface)

Table V. Comparison of Predicted Responses with Experimental Responses

Pellet size fraction (mm)	Response measured	Predicted response	Experimental response	Absolute deviation	Normalized deviation (%)
1.00–1.40	Agg (%)	0.16	0.04	+0.12	+2.11
	E_c (%)	97.27	103.57	−6.30	−7.42
1.40–2.00	Agg (%)	0.02	0.00	+0.02	+0.63
	DSA_{small} (μg/mm^2)	1.12	1.03	+0.09	+9.19
	DSA_{large} (μg/mm^2)	1.53	1.48	+0.05	+3.56
2.00–2.80	Agg (%)	0.03	0.00	+0.03	+0.93
	E_c (%)	96.51	90.65	+5.86	+6.88

were compared with the experimental responses previously obtained. For the 1.00–1.40 mm pellet size fraction, responses from the condition of spray rate 4 mL/min, batch size 120 g and plenum pressure 1,500 mm WC were used for comparison. For the 1.40–2.00 mm and 2.00–2.80 mm pellet size fractions, responses from the condition of spray rate 8 mL/min, batch size 120 g and plenum pressure 1,500 mm WC were used. Table V shows the comparison of predicted responses with experimental responses. Absolute deviation values were calculated by taking the difference between predicted and experimental responses. Deviation values were normalized against mean experimental responses of all coating runs within the particular pellet size fraction and expressed as a percentage. In order to statistically determine the prediction error, it will be necessary to validate the optimized conditions by performing more repeats.

The largest normalized deviation observed was 9.19%. Deviations of predicted responses from experimental responses could be attributed to poor fit of some of the models applied for prediction where R^2 values were less than 70% (Table IV). The inadequate model fit could arise from other factors which were not considered within the factorial design. For instance, the change in pellet flow patterns with different process conditions and some premature escape of pellets from the coating chamber might have contributed to errors in the prediction model. Despite the deviations observed, the applied models provided reasonable prediction of the expected responses.

Pellet Flow Patterns

During tablet coating using the Supercell™ coater (Fig. 1a), air jets at the periphery of the spray nozzle first direct the tablets towards the nozzle where they are exposed to the spray of coating dispersion. The partially coated tablets are then pneumatically lifted upwards and away from the spray zone by the upward swirling airflow following which they descend along the periphery of the coating chamber before repeating the cycle again (15). Interestingly, the pellet flow patterns observed in this study were distinctively different from that described for tablet coating.

In the presence of fluidizing air, the pellets achieve its terminal velocity (V_t) when the downward force of gravity (F_g) is balanced by the upward force of drag (F_d) and buoyancy (F_b). In a typical fluid bed system, the air flowing through a bed of particles exerts a drag force upon the particles resulting in a pressure drop ($\triangle P$) across the bed. $\triangle P$ is magnified when the approach air velocity is increased (16). In addition, F_d and F_b will also increase, causing the pellet bed to expand and bed voidage to increase (17). The reduced resistance to the air flow will help to set the pellets in motion. The mathematical equations representing the relationships among the forces described herein are listed below:

$$F_g = F_b + F_d \tag{5}$$

$$F_g = (\pi/6)d^3\rho_s g \tag{6}$$

$$F_b = (\pi/6)d^3\rho g \tag{7}$$

$$F_d = C_d\rho_s^{\frac{1}{2}} V_t^2 A \tag{8}$$

$$V_t^2 = (4gd/3C_d)[(\rho_s - \rho)/\rho] \tag{9}$$

$$\Delta P = g[m/\rho_s S_b(\rho_s - \rho)] \tag{10}$$

where d is the diameter of the spherical object, g is gravitational acceleration, ρ_s is the density of pellets, ρ is the density of air, C_d is the drag coefficient (0.47 for spheres), V_t is the terminal velocity, A is the projected cross-sectional area of the sphere ($\pi d^2/4$), m is the pellet mass and S_b is the cross-sectional area of the pellet bed.

The V_t of the pellet changes due to the properties of the fluidizing air, the mass of the pellet and its projected cross-sectional surface area. Therefore, for larger pellets with greater surface area and larger mass, V_t is larger. Consequently, the larger pellets will require a larger $\triangle P$ to achieve effective fluidization. In addition, an overall denser and heavier pellet bed will also require a larger $\triangle P$ for fluidization. Three types of fluidization configurations are commonly reported (18,19). In the first configuration, the approach velocity is smaller than the minimum fluidization velocity and a fixed bed is observed. In the second configuration, the approach velocity is intermediate between the minimum fluidization velocity and V_t. The

Fig. 7. Schematic diagrams showing **a** 'central spout', **b** 'swirling' and **c** 'cyclical V-shaped' pellet flow patterns. *Arrows* indicate general direction of pellet movement

a **'Central spout' pellet flow pattern – Low extent of pellet fluidization/Δ P**

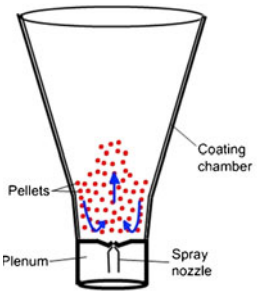

Pellets drawn towards the spray nozzle from the peripheral bed and propelled upwards as a central spout

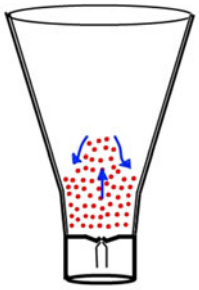

Pellets returning to the peripheral bed

b **'Swirling' pellet flow pattern – Moderate extent of pellet fluidization/Δ P**

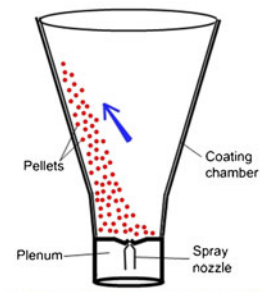

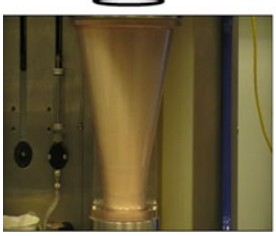

Pellets propelled towards the left side of coating chamber

Pellets propelled towards the back of the coating chamber

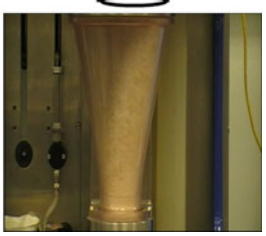

Pellets propelled towards the right side of the coating chamber

c **'Cyclical V-shaped' pellet flow pattern – High extent of pellet fluidization/Δ P**

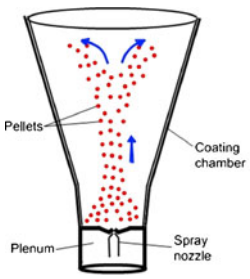

Pellets propelled towards the back of the coating chamber and diverge

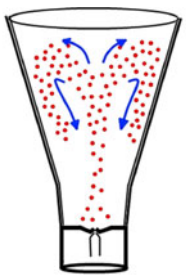

Pellets diverging into two cyclical flows

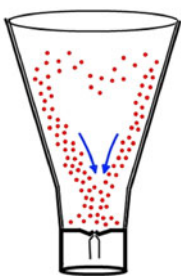

Pellets converging at the front of the coating chamber

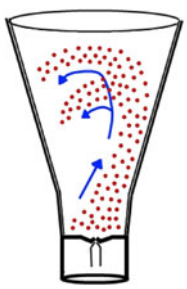

Pellet flow pattern - side view

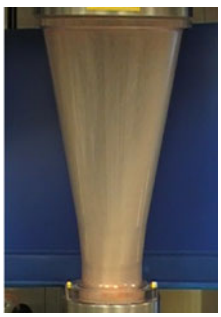

upward forces are sufficient to support the weight of the pellets and a stable fluidized bed is obtained. In the last configuration, the approach velocity is much greater than V_t and a pneumatically mobilized bed is obtained with entrainment of pellets in the exhausting fluidized air.

When pellet coating was performed in the Supercell™ coater, different pellet flow patterns were observed as a function of the plenum pressure, batch size and size of pellets coated. These factors influenced $\triangle P$ and V_t which can affect the fluidization tendencies and patterns of the pellets. At lower extents of pellet fluidization/$\triangle P$ (*i.e.*, a low plenum pressure and/or a large batch size), pellet flow generally assumed a 'central spout' flow pattern. This type of pellet flow pattern is illustrated in Fig. 7a. In this study, this pellet flow pattern was apparent only when the pellets of size fraction 2.00–2.80 mm were coated. This fluidization configuration was characterized by the persistence of a slow, downward-flowing pellet bed at the periphery of the coating chamber and was similar to the pattern of fluidization seen in the Wurster coating process which was reported to resemble a spouted bed (6). Pellets were drawn from the peripheral pellet bed towards the centrally located spray nozzle and propelled upwards to form a central spout before returning to the peripheral bed. As the pellet bed at the periphery of the chamber was minimally fluidized, higher Agg was observed. Increased pellet contact within this bed prompted the formation of agglomerates. This was similar to the 'downbed' region in the Wurster coating process where agglomerative tendencies are known to be high (7).

It was interesting to note that moderate extents of pellet fluidization/$\triangle P$ (*i.e.*, a moderate plenum pressure with a moderate batch size) were associated with a 'swirling' flow pattern. This was in contrast to the bubbling or boiling bed typically seen in fluid bed processes. In the Supercell™ coater, all the pellets were propelled towards the wall of the coating chamber in one general direction at any one point in time. In the next instant, the pellets were propelled towards another direction adjacent to the first. This continued cyclically without intermissions or breaks. When the Supercell™ coater was viewed top-down, the pellet load appeared to be moving in a clockwise 'swirling' pattern. This 'swirling' pellet flow pattern, as illustrated in Fig. 7b, is a direct result of the air distribution plate which was designed such that the ducts encircling the spray nozzle (Fig. 1) could channel the air at an angle and modify its flow pattern. This swirling airflow imparted extra momentum to the pellets being coated and minimized pellet agglomeration.

At high extents of pellet fluidization/$\triangle P$ (*i.e.*, a high plenum pressure and/or a small batch size), a 'cyclical V-shaped' flow pattern was observed with a prevalent central channel as pellets were pushed away from the central swirling air column. Here, the pellets were rapidly propelled towards the back of the coating chamber in one general direction with subsequent divergence towards the left and the right. The pellets then cycled back towards the front of the coating chamber where they converged. The two rapid cyclical flows which repeatedly diverged and converged formed a 'V-shaped' appearance. The 'cyclical V-shaped' pellet flow pattern is illustrated in Fig. 7c. This configuration led to better drying which would reduce the extent of pellet agglomeration but at the same time, encourage the premature escape of pellets from the coating chamber. The greater extents of fluidization also led to greater spray-drying and loss of coating material.

Interestingly, the optimized conditions for the three different pellet size fractions employed in this study corresponded to the 'swirling' pellet flow pattern. The 'swirling' pellet flow pattern was found to result in good outcomes for both Agg and E_c. In contrast, the 'central spout' pellet flow pattern resulted in a higher Agg while the 'cyclical V-shaped' pellet flow pattern resulted in greater material losses.

CONCLUSION

It is feasible to coat pellets using the Supercell™ coater. Through a systematic factorial design analysis, a better understanding and appreciation of the effects of equipment and material-related factors on the pellet coating process in the new coater was achieved. The pellet coating process was further optimized for three different size fractions of pellets and high coating efficiencies coupled with low degrees of pellet agglomeration were attained. Depending on the coating conditions employed, different pellet flow patterns were apparent and this led to variations in process efficiency and product quality. Amongst the different flow patterns observed, a 'swirling' pellet flow pattern generally brought about improved product quality.

Despite the promise shown by the Supercell™ coater for pellet coating, the current design of the coater will need to undergo certain design modifications in order to more effectively contain the pellets during the coating process. This is to prevent the premature escape of small pellets from the coating chamber and their subsequent loss in the exhaust which will adversely affect product quality and yield. Additionally, future studies can focus on extending the findings of this study to the coating of pellets for sustained- or controlled-release applications.

ACKNOWLEDGMENTS

The authors would like to thank GEA Pharma Systems (UK) for the loan of the Supercell™ coater and Colorcon (Asia) for providing the coating materials used in this study. GEA-NUS PPRL (N-148-000-008-001) and SERC Grant No. 102 169 0049 (R-148-000-157-305) are also acknowledged for the financial support provided.

REFERENCES

1. Heng PWS. Pelletization and pellet coating. 15th International Symposium on Microencapsulation; Parma, Italy; 2005.
2. Porter SC. Coating of tablets and multiparticulates. In: Aulton ME, editor. Aulton's pharmaceutics: the design and manufacture of medicines. 3rd ed. London: Churchill Livingstone; 2007. p. 500–14.
3. Chan LW, Tang ESK, Heng PWS. Comparative study of the fluid dynamics of bottom spray fluid bed coaters. AAPS PharmSciTech. 2006;7(2):E1–9.
4. Heng PWS, Chan LW, Tang ESK. Use of swirling airflow to enhance coating performance of bottom spray fluid bed coaters. Int J Pharm. 2006;327(1–2):26–35.
5. Walter KT (inventor). Apparatus for coating solid particles. United States 718 764. 1998.

6. Jones D. Air suspension coating for multiparticulates. Drug Dev Ind Pharm. 1994;20(20):3175–206.
7. Christensen FN, Bertelsen P. Qualitative description of the Wurster-based fluid-bed coating process. Drug Dev Ind Pharm. 1997;23(5):451–63.
8. Cahyadi C, Heng PWS, Chan LW. Optimization of process parameters for a quasi-continuous tablet coating system using design of experiments. AAPS PharmSciTech. 2010;12(1):119–31.
9. Birkmire AP, Liew CV. An accurate method of coating tablets with active pharmaceutical ingredients. 5th European Coating Symposium 2003 Proceedings. 2003:279–84.
10. Birkmire AP, Liew CV. Tablet coating in the novel Supercell coater: Evaluation of colour uniformity. American Association of Pharmaceutical Scientists Annual Meeting 2004 Poster session 2004.
11. Tang ESK, Wang L, Liew CV, Chan LW, Heng PWS. Drying efficiency and particle movement in coating—impact on particle agglomeration and yield. Int J Pharm. 2008;350(1–2):172–80.
12. Teunou E, Poncelet D. Batch and continuous fluid bed coating—review and state of the art. J Food Eng. 2002;53(4):325–40.
13. Wesdyk R, Joshi YM, Jain NB, Morris K, Newman A. The effect of size and mass on the film thickness of beads coated in fluidized bed equipment. Int J Pharm. 1990;65:69–76.
14. Sudsakorn K, Turton R. Nonuniformity of particle coating on a size distribution of particles in a fluidized bed coater. Powder Technol. 2000;110(1–2):37–43.
15. Walter KT, Neidlinger MA (inventors). Apparatus for coating tablets. United States 6,209,4798. 2001.
16. Dixit R, Puthli S. Fluidization technologies: aerodynamic principles and process engineering. J Pharm Sci. 2009;98 (11):3933–60.
17. Khani MH. Models for prediction of hydrodynamic characteristics of gas-solid tapered and mini-tapered fluidized beds. Powder Technol. 2011;205(1–3):224–30.
18. Marzocchella A, Salatino P, Di Pastena V, Lirer L. Transient fluidization and segregation of binary mixtures of particles. AIChE J. 2000;46(11):2175–82.
19. Fan XF, Yang ZF, Parker DJ. Impact of solid sizes on flow structure and particle motions in bubbling fluidization. Powder Technol. 2011;206(1–2):132–8.